Vibration from a Shaft-Bearing-Plate System Due to an Axial Excitation of Helical Gears

Chan IL Park

*Department of Precision Mechanical Engineering, Kangnung National University,
Gangneung, Gangwon-do 210-702, Korea*

In this paper, a simplified model is studied to predict analytically the vibration from the helical gear system due to an axial excitation of helical gears. The simplified model describes gear, shaft, bearing, and housing. In order to obtain the axial force of helical gears, the mesh stiffness is calculated in the load deflection relation. The axial force is obtained from the solution of the equation of motion, using the mesh stiffness. It is used as a longitudinal excitation of the shaft, which in turn drives the gear housing through the bearing. In this study, the shaft is modeled as a rod, while the bearing is modeled as a parallel spring and damper only supporting longitudinal forces. The gear housing is modeled as a clamped circular plate with viscous damping. For the modeling of this system, transfer matrices for the rod and bearing are used, using a spectral method with four pole parameters. The model is validated by finite element analysis. Using the model, parameter studies are carried out. As a result, the linearized dynamic shaft force due to the gear excitation in the frequency domain was proposed. Out-of-plan displacement from the forced vibrating circular plate and the renewed mode normalization constant of the circular plate were also proposed. In order to control the axial vibration of the helical gear system, the plate was more important than the shaft and the bearing. Finally, the effect of the dominant design parameters for the gear system can be investigated by this model.

Key Words : Helical Gear, Circular Plate, Vibration, Spectral Method, Receptance Method

Nomenclature

a : The radius of the circular plate
C : Damping
e : Tooth error
E : Modulus of elasticity
F : Force
I_m : Modified Bessel functions of the first kind of order m
J_m : Bessel functions of the first kind of order m
j : Complex number
J : Mass moment of inertia
h : Plate thickness

K : Stiffness
k : Wave number
l : The length of the shaft
M : Mass
R_b : Base circle radius
t : Time
T : Torque
U : Displacements
δ : Kronecker delta
ρ : Density
ν : Poisson's ratio
ξ : Damping coefficient
β_b : Base helix angle
θ : Rotation angle

Subscripts

1 : Driving gear
2 : Driven gear
B : Bearing

* Corresponding Author,
  E-mail : pci@kangnung.ac.kr
  TEL : +82-33-640-2392; **FAX** : +82-33-640-2244
  Department of Precision Mechanical Engineering, Kangnung National University, Gangneung, Gangwon-do 210-702, Korea. (Manuscript **Received** March 30, 2006; **Revised** September 1, 2006)

G ： Gear
P ： Plate
S ： Shaft

Superscripts
• ： Dot, time derivative
－ ： Average

1. Introduction

The helical gear system is widely used in the power transmission mechanical system, because of low noise characteristics of helical gear, as the gear system comes to the high speed, the gear noise and vibration become more important. Analysis capability to predict the noise of not only gears itself but also the helical gear system is required.

The vibration from the gear meshing is transmitted to the gear housing through the shaft and bearing. Housing vibration radiates noise in air. The gear noise is caused by the structure-borne noise. Therefore, reliable gear system modeling for the transmission of the gear vibration is required. As a related research, Ozguven and Houser reviewed and classified the mathematical models used in dynamics of gear system which consisted of gears, bearings, and shaft (Ozguven and Houser, 1998). Lim and Singh examined a generic gearbox containing one spur gear pair using the statistical energy analysis with emphasis on the vibratory energy flow through rolling element bearings (Lim and Singh, 1991). Jacobson tried to predict the radiation efficiency using the rectangular plate (Jacobson et al., 1996). Misun predicted the acoustic pressure using FE analysis of gearbox housing (Misun and Prikryl, 1995). Sabot computed the noise by using the finite element modeling of one rectangular face of gearbox and Rayleigh integral (Sabot and Perret-Liaudet, 1994). Rautert calculated the bearing force and tried to relate the force to the noise (Rautert, 1989). Park tried to predict the sound pressure of shaft-plate system as the model problem of gear system (Park and Grosh, 1998 ; Park, 2000). As a part of the effort to predict analytically the noise for the helical gear system, vibration model for the gear system is investigated. Gear system is modeled as a shaft-bearing-plate system. Vibration of the circular plate with viscous damping is derived. In order to complete the connection between the bearing and the plate, the force balance equation and the displacement continuity equation are used. The equation for the natural frequencies of the system is derived by receptance method. The model is validated by finite element analysis.

Using the model, transmission of force and displacement due to axial excitation of helical gear is investigated. Parameter studies of the system such as load, plate thickness and so on are also investigated.

2. Mathematical Models

The model used in this analysis consists of the helical gear pair, shaft, bearing, and plate as shown in Fig. 1. Axial excitation of helical gear pair is assumed to transmit to the shaft. Therefore, only longitudinal excitation of shaft is considered. The shaft is modeled as a rod and the bearing as a parallel spring and dashpot.

Gear housing is modeled as a damped thin circular plate connected with shaft off the center of the plate. To model the system, a set of four pole parameters is used. Such modeling is similar in spirit to spectral element formulation as described in Doyle (1997). The input side of the element vibrates sinusoidally with a displacement U_1 in response to applied force F_1. At the output side,
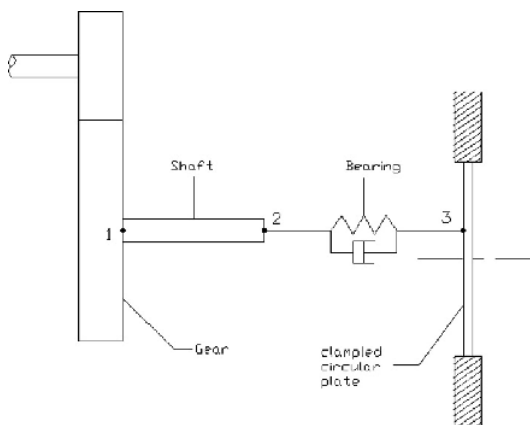

Fig. 1   Mathematical model

there exists a force F_2 and a displacement U_2, which result from input force and displacement. Parameters that relate the input force and displacement to the output force and displacement are known as four–pole parameter (Snowdon, 1971). In this analysis, axial excitation of helical gear is calculated. And the transfer matrix of an element, which consists of four–pole parameters, is connected in series to obtain the force transmission from the shaft to the plate. Finally, Out–of–plane displacement for the thin circular plate with viscous damping and the mode normalization constant are derived.

2.1 Gear

An axial vibration of helical gear is highly related to the rotational vibration, which is caused by the transmission error of gears and leads to the vibration in the rotational direction of gear system and the important peaks of axial vibration correspond to those of rotational one. Therefore, this study calculates the force due to rotational vibration and it is transformed into axial forces by the base helix angle.

Figure 2 is the gear model of the rotational direction used in this analysis. Rotational vibration is formulated as shown in Equation (1) and it includes variable mesh stiffness, mesh damping and gear errors.

$$M\ddot{x}+2\xi_G\sqrt{M\bar{K}_G}\dot{x}+K_G(t,x)x = F_G+F(t,x) \tag{1}$$

where

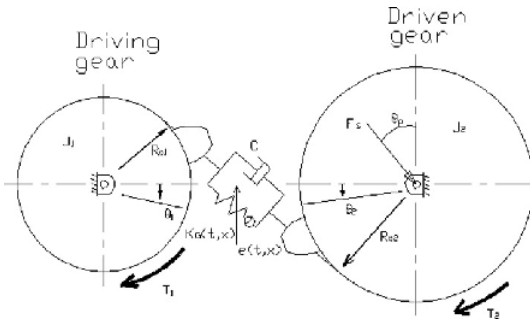**Fig. 2** Vibration model of the helical gear

$$x=R_{b1}\theta_1-R_{b2}\theta_2,\ F(t,x)=\sum_j K_{Gj}e_j,$$

$$F_G=T/R_{b1},\ M=\frac{J_1J_2}{J_1R_{b2}^2+J_2R_{b1}^2}.$$

This equation can be transformed into the normalized linear equation with non-dimensional variables as follows (Cai and Hayashi, 1994).

$$\ddot{X}+2\xi_G\omega_n\dot{X}+\omega_n^2X=\omega_n^2Y(t) \tag{2}$$

where

$$X=x/x_{st},x_{st}=F_G/\bar{K}_G,\ \omega_n=\sqrt{\bar{K}_G/M},$$

$$Y(t)=y(t)/x_{st},\ y(t)=\frac{F_G+F(t,x)}{K_G(t,x)}.$$

The periodic forcing function $Y(t)$ can be expressed in terms of harmonic functions with the phase ϕ as

$$Y(t)=Y_o+\sum_{i=1}^{\infty}Y_i\sin(i\omega t+\phi_i) \tag{3}$$

The steady state response with the phase φ is given by

$$X=Y_o+\frac{\sum_{i=1}^{\infty}\omega_n^2Y_i\sin(i\omega t+\phi_i-\varphi_i)}{\sqrt{(\omega_n^2-(i\omega)^2)^2+(2\xi_G\omega_ni\omega)^2}} \tag{4}$$

The response in the rotational direction is transmitted to the shaft by damping force and mesh stiffness force. Multiplying the shaft force in the rotational direction by the tangent of the base helix angle, the shaft force is transformed into the axial shaft force as follows.

$$F_s=\frac{\sum_{i=1}^{\infty}\bar{K}_GY_i\sqrt{(2\xi_G\omega_ni\omega)^2+\omega_n^4}\sin(i\omega t+\phi_i-\varphi_{si})x_{st}\tan\beta_b}{\sqrt{(\omega_n^2-(i\omega)^2)^2+(2\xi_G\omega_ni\omega)^2}}$$
$$+\bar{K}_GY_ox_{st}\tan\beta_b \tag{5}$$

2.2 Shaft

Since the shaft is modeled as a rod, the governing equation in the rectilinear coordinate x for the rod is given by

$$\frac{\partial}{\partial x}\left[EA(x)\frac{\partial u(x,t)}{\partial x}\right]=\rho A(x)\frac{\partial^2 u(x,t)}{\partial t^2} \tag{6}$$

where $EA(x)$ is the axial stiffness, $\rho A(x)$ is the axial density and $u(x,t)$ is the axial displacement. Since the uniform shaft is considered, the modulus and area are constant. Assuming that a

solution is $u(x,t) = U(x) e^{j\omega t}$, the general solution of wave equation is obtained. Applying the input force and displacement and the output force and displacement to the solution, the force F_2 and the displacement U_2 at node 2 and the four-pole parameters are given by

$$\begin{Bmatrix} F_2 \\ U_2 \end{Bmatrix} = \begin{bmatrix} \alpha_{11}^1 & \alpha_{12}^1 \\ \alpha_{21}^1 & \alpha_{22}^1 \end{bmatrix} \begin{Bmatrix} F_1 \\ U_1 \end{Bmatrix} \tag{7}$$

where

$$\alpha_{11}^1 = \cos(k_r l), \quad \alpha_{12}^1 = z\omega \sin(k_r l),$$
$$\alpha_{21}^1 = -\sin(k_r l)/z\omega, \quad \alpha_{22}^1 = \cos(k_r l),$$
$$c_r = \sqrt{E/\rho}, \quad k_r = \omega/c_r, \quad z = \sqrt{E\rho}A.$$

2.3 Bearing

Since the bearing is modeled as the parallel spring and dashpot, the bearing force F_{3B} and the bearing displacement U_{3B} at node 3 and the four-pole parameters of the parallel spring and dashpot element are given by

$$\begin{Bmatrix} F_{3B} \\ U_{3B} \end{Bmatrix} = \begin{bmatrix} \alpha_{11}^2 & \alpha_{12}^2 \\ \alpha_{21}^2 & \alpha_{22}^2 \end{bmatrix} \begin{Bmatrix} F_2 \\ U_2 \end{Bmatrix} \tag{8}$$

where

$$\alpha_{11}^2 = 1, \quad \alpha_{12}^2 = 0, \quad \alpha_{21}^2 = -1/(K_B + jC_B), \quad \alpha_{22}^2 = 1.$$

2.4 Clamped damped circular plate

Governing equation of circular plate in the polar coordinate with viscous damping subject force F_{3P} at r_o and θ_o is given by (Morse and Ingard, 1968)

$$D\nabla^4 w + C_P \frac{\partial w}{\partial t} + \rho h \frac{\partial^2 w}{\partial t^2} = F_{3P}\delta(r - r_o)\delta(\theta - \theta_o)/r \tag{9}$$

where $D = Eh^3/12(1-\nu^2)$ and $w(r,\theta,t)$ is the out-of-plane displacement.

Assuming that the solution is $w(r,\theta,t) = W(r,\theta)e^{j\omega t}$, the spectral form for this equation is obtained. Modal expansion to derive the forced response of the plate is used. By solving the characteristic equation of the undamped circular plate satisfied with the clamped boudary condition, eigenvalues and the corresponding normal mode are calculated. By substituting the normal mode

equation into the spectral equation and using the orthogonality of mode, the out-of-plane displacement of the plate is obtained by

$$w(r,\theta,t)$$
$$= \sum_{m=0}^{\infty}\sum_{n=1}^{\infty} \frac{F_{3P}H_{mn}(\beta_{mn}r_o)H_{mn}(\beta_{mn}r)}{\varepsilon\pi a^2 D\Lambda_{mn}(\beta_{mn}^4 - \beta^4)}\cos(m\theta - m\theta_o)e^{j\omega t} \tag{10}$$

where

$$H_{mn}(\beta_{mn}r) = J_m(\beta_{mn}r) - \frac{J_m(\beta_{mn}a)}{I_m(\beta_{mn}a)}I_m(\beta_{mn}r),$$

$$\beta_{mn}^4 = (\omega_{mn}^2 \rho h)/D, \quad \beta^4 = (\omega^2 \rho h - j\omega C_P)/D.$$

If $m > 0$, $\varepsilon = 1$, and if $m = 0$, $\varepsilon = 2$. Λ_{mn} is the mode normalization constant and lead to accurate natural frequencies of the system. In this paper, it is derived by $\Lambda_{mn} = J_m^2(\beta_{mn}a)$.

2.5 Plate forces and the natural frequencies of the system

The rod and the bearing are connected in series. Therefore, the bearing force is calculated by multiplying the transfer matrix for the rod and the transfer matrix for the bearing like Eq. (11).

$$\begin{Bmatrix} F_{3B} \\ U_{3B} \end{Bmatrix} = \begin{bmatrix} \alpha_{11}^2 & \alpha_{12}^2 \\ \alpha_{21}^2 & \alpha_{22}^2 \end{bmatrix}\begin{bmatrix} \alpha_{11}^1 & \alpha_{12}^1 \\ \alpha_{21}^1 & \alpha_{22}^1 \end{bmatrix}\begin{Bmatrix} F_1 \\ U_1 \end{Bmatrix} = \begin{bmatrix} \alpha_{11} & \alpha_{12} \\ \alpha_{21} & \alpha_{22} \end{bmatrix}\begin{Bmatrix} F_1 \\ U_1 \end{Bmatrix} \tag{11}$$

Since the plate and the bearing is joined, the force balance Eq. (12) and the displacement continuity Eq. (13) at the connected point are used.

$$F_{3B} = F_{3P} \tag{12}$$

$$U_{3B} = U_{3P} \tag{13}$$

Here F_{3P} is the force of the plate and U_{3P} is the displacement of the plate at node 3 located r_o and θ_o on the plate. Using Eq. (10), it is expressed by

$$U_{3P} = W(r_o, \theta_o) = F_{3P}/K_P \tag{14}$$

where

$$1/K_P = \sum_{m=0}^{\infty}\sum_{n=1}^{\infty} \frac{\{H_{mn}(\beta_{mn}r_o)\}^2}{\varepsilon\pi a^2 D\Lambda_{mn}(\beta_{mn}^4 - \beta^4)}$$

From the Eqs. (11) ~ (14), the relation between U_1 and F_1 is given by

$$U_1 = \frac{\alpha_{21} - \alpha_{11}/K_P}{\alpha_{12}/K_P - \alpha_{22}}F_1 \tag{15}$$

Substitututing the Eq. (15) into Eq. (11), the force

excited at the plate in Eq. (12) is given by

$$F_{3P} = \frac{\alpha_{11}\alpha_{22} - \alpha_{12}\alpha_{21}}{\alpha_{22} - \alpha_{12}/K_P} F_1 \qquad (16)$$

In order to calculate the natural frequencies of the gear system, the receptance method (Bishop and Johnson, 1960 ; Sodel, 1993) is used. The definition of the receptance method is given by

$$\frac{U_{3B}}{F_{3B}} = \frac{U_{3P}}{F_{3P}} \qquad (17)$$

Substituting Eqs. (11) and (14) into Eq. (17) at the free vibration condition, the equation for natural frequencies of the system is obtained by

$$\frac{\alpha_{22}}{\alpha_{12}} = \frac{1}{K_P} \qquad (18)$$

3. Results and Discussion

For the numerical examples, the helical gear data of Table 1 are used. Steel shaft with the diameter of 20 mm and the length of 265 mm and an aluminum alloy circular plate with a diameter of 400 mm and thickness 5 mm are used. The transmitted load of the gear is 136 N. All calculation is performed by MATLAB on personal computer. The material of gears is steel and gears assume to have the true involute profiles without lead errors and lead crowning. The mesh stiffness of helical gears is obtained by an in-house program (Park and Lee, 1993 ; Park and Kim, 2002), which is calculated by the load-deformation equation along the contact line.

Table 1 The data of helical gears

	Pinion	Gear
Normal module	2.25	
Normal pressure angle (deg)	17.5°	
Center distance (mm)	127	
Whole depth (mm)	6.6	
Helix angle (deg)	28°	
Number of teeth	48	50
Outside diameter (mm)	130.36	135.26
Pitch diameter (mm)	122.32	127.41
Amount of add. mod.(mm)	1.17	1.07

To calculate the axial excitation force of the helical gear transmitted to the shaft, the linearized equation of motion in the rotational direction should be solved. For the damping of the equation, the damping coefficient of 0.07 mentioned by most gear researchers is used.

An axial stiffness of the taper roller bearing uses the equation of the reference (Gargiulo, 1980). Bearing stiffness varies very little between static and dynamic conditions (Kraus et al., 1987). Thus, it is sufficient to obtain the static stiffness of the bearing. For the bearing stiffness, the bearing data of SKF 30204J2 is used. The damping of bearing is obtained by the modal testing of the experimental apparatus for the bearing as shown in Fig. 3. Under the axial force $F = 136$ N, impulse hammer is excited in the axial direction. For the modal testing, I-deas software and Agilent E8408A
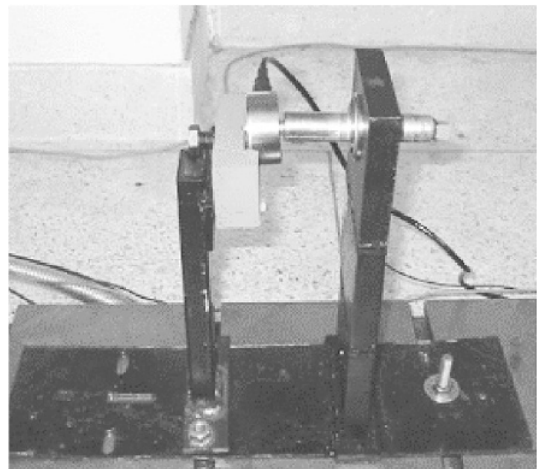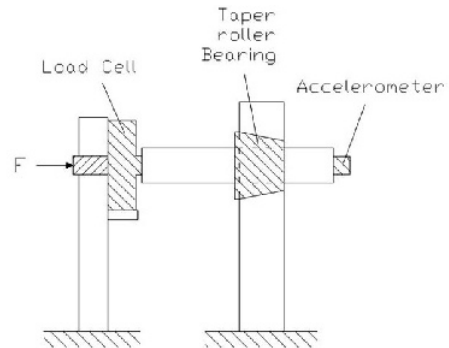

Fig. 3 Experimental apparatus used to measure the bearing parameter

VXi mainframe are used. At the frequency of 57 Hz with an axial mode, damping ratio of 4.116% is obtained. As a result, bearing damping of 142 N/m/sec is used for the numerical example (Zaveri, 1994).

The damping of plate is also obtained by the modal testing of the fixed aluminum circular plate as shown in Fig. 4. For the modal testing, impulse hammer is excited and the same software and front end as the bearing experiment are used. At the first natural frequency of 250 Hz, the damping ratio of 1.562% is obtained. From the results, the damping of 744 N/m/sec is used for the numerical example.
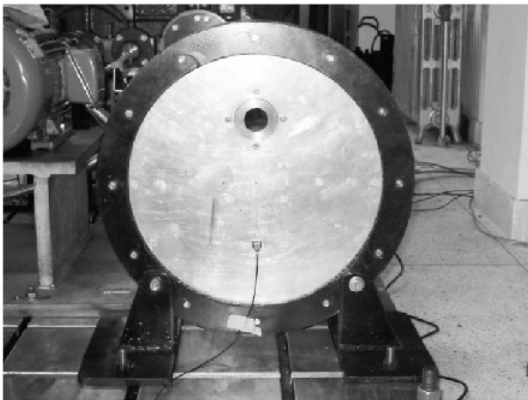
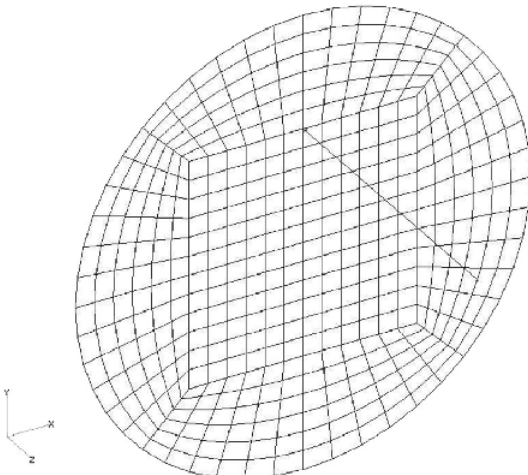**Fig. 4** Experimental apparatus used to measure plate damping

Fig. 5 Finite element modeling

The circular plate is connected with the bearing and shaft, which is located at the position of (r_o, θ_o) on the plate equal to $(0.1, 90°)$. In order to obtain the out-of-plane displacement of plate and sound pressure, 25 modes $(m=4, n=5)$ from 319 Hz $(m=0, n=1)$ to 14,567 Hz $(m=4, n=5)$ are used.

For validation of the model, finite element analysis is carried out. The commercial software NASTRAN for Window is used. Shaft is modeled by the rod element and the bearing is modeled by the spring element with stiffness of 6.84×10^7 N/m. The circular plate is modeled by the four node rectangular element. Fig. 5 shows the finite element modeling. Natural frequencies in the simulation is calculated by Eq. (18). Natural frequencies of the finite element analysis and simulation are compared in Table 2. As a result, the difference of natural frequency is no more than 2%. The mode normalization constant proposed in this paper is different to Morse and Ingard's equation. If their equation is used, first natural frequency is 460 Hz, which is different from the result of FE analysis. Therefore, out of displacement for the circular plate and the mode normalization constant derived is correct and validation of the model is confirmed.

The axial shaft force calculated by the Eq. (5) is shown in the frequency domain as Fig. 6. It is used as the exciting force of the shaft-bearing-plate system. The frequency indicates the exciting one relative to the rotational speed. It shows the subharmonic peaks by the parametric excitation of gear. Figure 7 is the bearing force transmitted to the plate. The force is calculated by F_{3B} of Eq. (8). In this figure, the peak associated with the axial shaft force of Fig. 4 isn't found. Many peaks

Table 2 Natural frequency comparison between FE anaysis and simulation

No	FE analysis	Simulation	Difference
1	221 Hz	225 Hz	1.80%
2	430 Hz	439 Hz	2.09%
3	873 Hz	887 Hz	1.60%
4	1220 Hz	1216 Hz	0.32%
5	1414 Hz	1437 Hz	1.62%

correspond to the peak of the plate and is related with natural frequencies of the plate. Because the bearing is joined with the plate by the bearing stiffness, the bearing forces are greatly dependent on the natural frequencies of the plate. In order to predict the more exact bearing behavior, the detail modeling of the bearing is needed.

Figure 8 shows the out–of–plane displacement of plate calculated at the position $(0.1, 0.)$, using these values. Figure 8 has peaks at the natural frequencies associated with plate modes $m = 0, 2$ and 4, which the choice of the calculation point determines the participation of modes. Therefore, plate modes are more important than shaft modes, and bearing modes in case of axial gear excitation.

In gear mechanics, the deformation is not linearly dependent on load. Load increase leads to the nonlinear change of mesh stiffness and bearing stiffness due to the contact deformation. The tooth error also leads to the nonlinear load–deformation relationship. Therefore, new mesh stiffness and bearing stiffness under the high normal transmitted load is calculated and the linearized shaft force is calculated under the given mesh stiffness. In order to investigate the effect of the high transmitted gear load, the two transmitted loads, 680 N and 1360 N, are applied and investigated in Fig. 9. As the load is increased by two times, the out–of–plane displacement of the circular plate increases. However, the increase of the
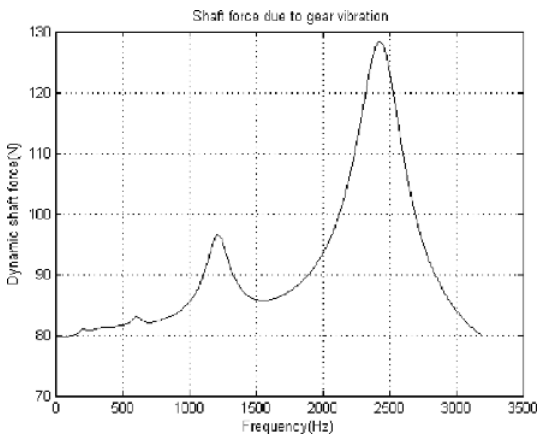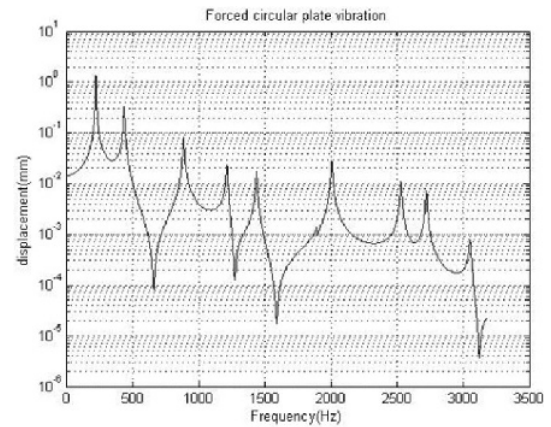

Fig. 6 Axial shaft force

Fig. 8 Out–of–plane displacement of the circular plate

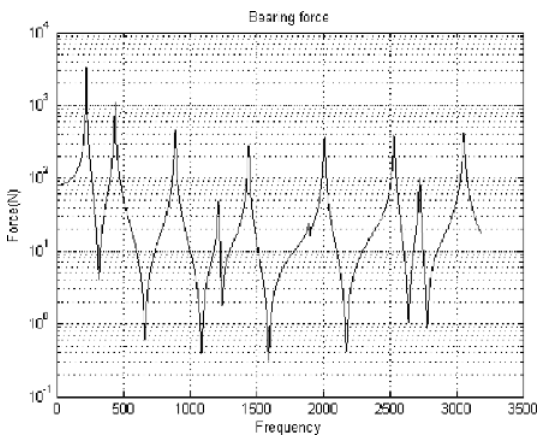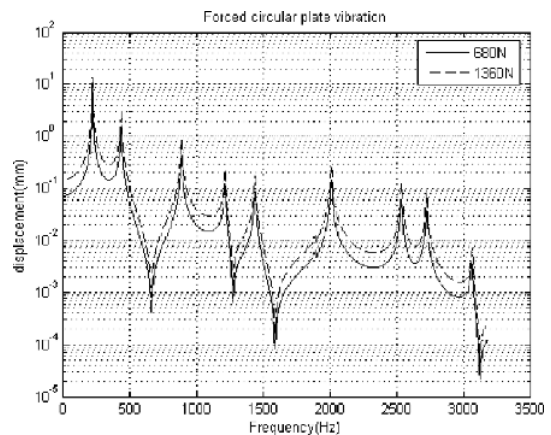**Fig. 7** Bearing force

Fig. 9 Out–of–plane displacement of the plate by the load change

gear load does not generate a dramatic change in the plate vibration.

Figure 10 is to investigate the effect of the vibration in case of the plate thickness 7 mm and 10 mm. While the plate of thickness 10 mm has five peaks in the 0~3180 Hz frequency range, the plate of 7 mm has seven peaks. The plate of 10 mm is smaller than the plate of 7 mm in the amplitude of the out-of-plane displacement, although the peaks move in the high frequency region. Therfore, thickening the thickness makes the plate to be stiff and less vibrant.

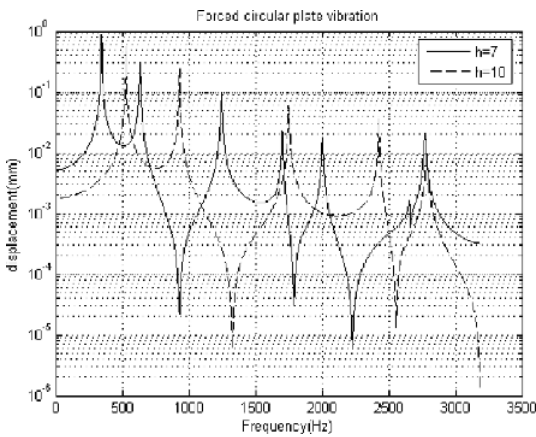The effect of the plate material change is investigated in Fig. 11. Three materials of the steel, the aluminum, and the magnesium with the material properties in Table 3 are compared. They show the differences between the frequency characteristics below 500 Hz and around 3 kHz. The magnesium plate has the lowest fundamental natural frequency while the steel plate has the high fundamental natural frequency. From 500 Hz to below 3 kHz, three materials have similar frequency characteristics. Although the magnesium as the exchange material of the aluminum for the weight reduction is used in the housing, the frequency characteristics don't have the great changes.

The effect of the variable nonlinear bearing stiffness by Gargiulo's equation and the fixed bearing stiffness of 68.4 MN/m is investigated in Fig. 12. Except for the high frequency region near 3 kHz, almost the same results show up. Figure 13 shows the effect of three different bearing stiffness. If the bearing stiffness of 6.84 MN/m is assumed to be used, the frequency characteristics is greatly changed at the high frequency region. However the bearing stiffness of 68.4 MN/m and 684 MN/m don't make a great difference. The

Fig. 10 Out-of-plane displacement of the plate by the plate thickness

Table 3 Material Properties

Materials	Density (kg/m³)	Poisson's ratio	Young's modulus (GPa)
Steel	7700	0.29	206
Aluminum	2700	0.33	71
Magnesium	1796	0.35	44.8
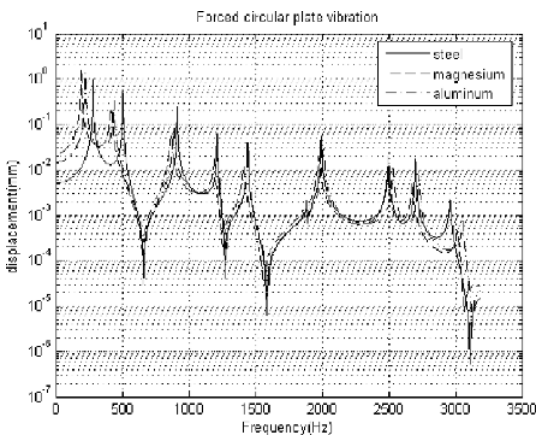
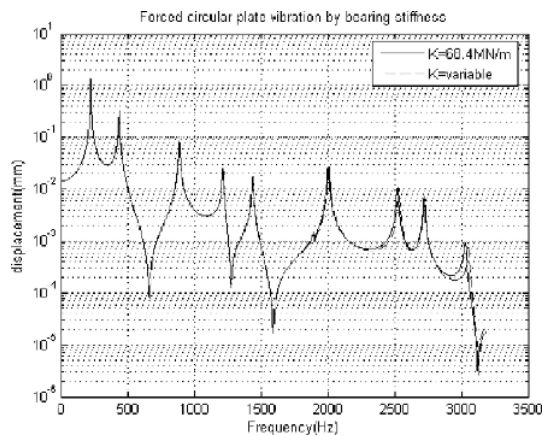**Fig. 11** Out-of-plane displacement of the plate by the plate material

Fig. 12 Comparison between the varible bearing stiffness and the constant bearing stiffness

application of the high bearing stiffness let the frequency characteristics move to the high frequency region.

Figure 14 shows the effect of the shaft diameters with the fixed bearing stiffness. Three shaft diameters of 20 mm, 30 mm, and 40 mm are investigated. The shaft diameter of 40 mm has the lowest fundamental natural frequency and the low vibration in the non-resonance area while 20 mm has the highest natural frequency and the high vibration in the non-resonance area. The big shaft diameter increases the mass of the system and leads to the low frequency. However, natural fequencies of three shaft diameters don't change at the more than 500 Hz.
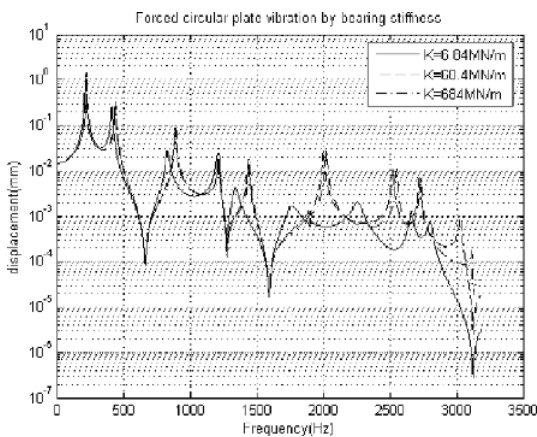

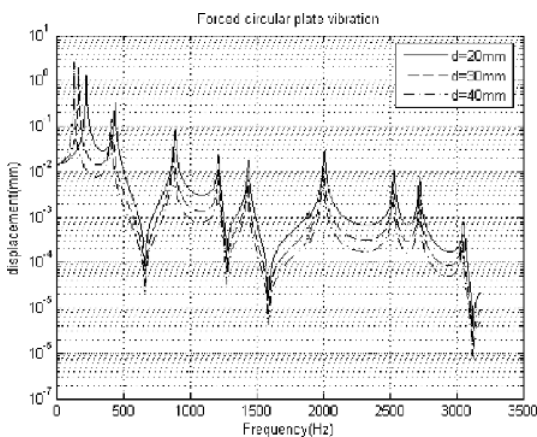**Fig. 13** Out-of-plane displacement of the plate by the bearing stiffness

Fig. 14 Out-of-plane displacement of the plate by shaft diameters

4. Summary and Conclusion

The vibration of shaft-bearing-plate system due to the axial excitation force of helical gears was studied. The four pole parameters for a rod and a spring were used to model the shaft and the bearing. The damped circular plate employed as a simple model of housing was used. The model was validated by finite element analysis. The important parameters of the bearing and plate were also measured by the specially designed experimental set-up. Using the model, parameter studies by numerical simulation were carried out. As a result, the following results were obtained.

(1) The linearized dynamic shaft force due to the gear excitation in the frequency domain was proposed.

(2) Out of displacement from the forced vibrating circular plate and the renewed mode normalization constant of the circular plate were proposed.

(3) In order to control the axial vibration of the helical gear system, the plate was more important than the shaft, and the bearing.

(4) The effect of the dominant design parameters for the gear system can be investigated by this model.

Acknowledgments

References

Bishop, R. E. D. and Johnson, D. C., 1960, *The Mechanics of Vibration*, Cambridge University Press, London.

Cai, Y. and Hayashi, T., 1994, "The Linear Approximated Equation of Vibration of a Pair of Spur Gears (Theory and Experiment)," *Journal of Mechanical Design*, Vol. 116, pp. 558~564.

Doyle, J. F., 1997, *Wave Propagation in Struc-*

tures, 2ed., Springer, NY.

Gargiulo, E. P. JR., 1980, "A Simple Way to Estimate Bearing Stiffness," *Machine Design*, July, pp. 107~110.

Graff, K. F., 1991, *Wave Motion in Elastic Solids*, Dover, NY.

Jacobson, M. F., Singh, R. and Oswald, F. B., 1996, "Acoustic Radiation Efficiency Models of a Simple Gear box," NASA TM-107226.

Kraus, J. et al., 1987, "In Situ Determination of Rolling Bearing Stiffness and Damping by Modal Analysis," *Journal of Vibration, Acoustics, Stress, and Reliability in Design*, Vol. 109, pp. 235~240.

Lim, T. C. and Singh, R., 1991, "Statistical Energy Analysis of a Gearbox With Emphasis on the Bearing Path," *Noise Control Engineering Journal*, Vol. 37, No. 2, pp. 63~69.

McLachlan, N. W., 1955, *Bessel Functions for Engineers*, 2nd ed., Oxford University, London.

Misun, V. and Prikryl, K., 1995, "Acoustic Response Modeling of the Mechanical Gearbox," *Gearbox Noise, Vibration, and Diagnostics*, MEP, pp. 153~162.

Morse, P. M. and Ingard, K. U., 1968, *Theoretical Acoustics*, McGraw-Hill, NY.

Ozguven, H. N. and Houser, D. R., 1998, "Mathematical Models Used in Gear Dynamics-A Review," *Journal of Sound and Vibration*, 121 (3), pp. 383~411.

Park, C. I. and Lee, J. M., 1993, "Load Transmission and Vibration Characteristics of Automobile Gear," SAE Paper 932917.

Park, C. I. and Grosh, Karl, 1998, "Radiated Noise From a Clamped Circular Plate-Shaft System," *ASME International Mechanical Engineering Congress, Recent Advances in Solids and Struc-*tures, Anaheim, CA, USA, pp. 199~204.

Park, C. I. and Kim, D. S., 2002, "Transmission Error Analysis of the Helical Gears for the Elevator," *Trans. of KSME, A*, Vol. 26, No. 12, pp. 2695~2702.

Park, C. I., 2000, "Analytical Procedure for Prediction of Radiated Noise From a Gear-Shaft-Plate System," *Proceedings of DETC'00*, DETC 2000/PTG-14444, USA.

Park, C. I., 2005, "Noise and Vibration From a Shaft-bearing-plate system due to an Excitation of Helical Gears," *Proceedings of Twelfth International Congress on Sound and Vibration*, Lisbon, Portugal.

Rautert, J. and Kollmann, F. G., 1989, "Computer Simulation of Dynamic Forces in Helical and Bevel Gear," *Proceedings of 1989 International Power Transmission and Gearing Conference*, USA, Vol. 1, pp. 435~446.

Sabot, J., Perret-Liaudet, J., 1994, "Computation of the Noise Radiated by a Simplified Gearbox," *Proceedings of 1994 International Gearing Conference*, UK, pp. 63-68.

Snowdon, J. C., 1971, " Mechanical Four-pole Parameter and Their Application," *Journal of Sound and Vibration*, Vol. 15, No. 3, pp. 307~323.

Snowdon, J. C., 1970, "Forced Vibration of Internally Damped Circular Plates with Supported and Free Boundaries," *The Journal of the Acoustical Society of America*, Vol. 47, No. 3, pp. 882~891.

Soedel, W., 1993, *Vibrations of Shells and Plates*, 2nd ed. Marcel Dekker, NY.

Zaveri, K.(ed), 1994, *B & K Technical Review*, No. 2, B & K, Denmark.